A novel control system design to improve LVRT capability of fixed speed wind turbines using STATCOM in presence of voltage fault

CrossMark

Hamed Heydari-doostabad [a], Mohammad Reza Khalghani [b], Mohammad Hassan Khooban [c,*]

[a] *Department of Electrical Engineering, Ferdowsi University of Mashhad, Mashhad, Iran*
[b] *Department of Electrical and Computer Engineering, University of Birjand, 97175/376 Birjand, Iran*
[c] *Institute of Electrical Engineering, Shahid Bahonar University, Shiraz, Iran*

ARTICLE INFO

ABSTRACT

The design and implementation of a new control system for reactive power compensation and mechanical torque, voltage regulation and transient stability enhancement for wind turbines equipped with fixed-speed induction generators (IGs) in power systems is presented in this study. The designed optimal linear quadratic regulator (LQR) controller provides an acceptable post fault performance for both small and large perturbations. Large disturbance simulations demonstrate that the designed controller enhances voltage stability as well as transient stability of the system during low-voltage ride-through transients and thus enhances the LVRT capability of fixed-speed wind generators. Further verifications based on detailed time-domain simulations are also provided. Calculations, simulations and measurements confirm how the increased STATCOM rating can provide an increased transient stability margin and consequently enhanced LVRT capability. A concept of critical clearing time has been introduced and its utility has been highlighted.

Introduction

WIND turbines are one of the renewable energy technologies that, today, face a growing progress. This developments cause rapid progress of economic and environmental issues [1]; therefore, the study about connecting the turbines to the grid is very important [2].

Many countries have their own grid codes which monitor the behavior of the wind turbines connected to the grid [3]. All network grid codes for wind turbines include requirements such as low-voltage ride-through capacity (LVRT), voltage control, power-quality and protection requirements. In 2005, LVRT requirement was introduced the wind turbine rotor speed try to achieve stability on the index which requires a certain voltage, an example of the voltage profile is shown in Fig. 1.

If a fault or voltage drop occurs at stator terminals of wind turbine generator, according to (1), electrical torque will decrease while mechanical torque still exists because wind keeps blowing. According to Eq. (2), these conditions will cause rotor speed to increase. If this voltage drop continues, it may cause rotor of turbine to accelerate and make rotor speed unstable.

$$T_e \propto v_s^2 \tag{1}$$

$$\frac{d}{dt}\omega_r = \frac{1}{J}(T_m - T_e) \tag{2}$$

The maximum voltage drop (either in terms of magnitude or in terms of time) which wind turbine is able to withstand without suffering from rotor speed instability is called wind turbine low voltage ride through capability.

Wind turbine technologies include Fixed and variable speed wind turbines [5]. Since fixed-speed turbines are easy to install, durable and cost-effective, nowadays, most of the installed turbines are chosen from this category [6]. In Iran, about 91 MW of installed wind turbines are fixed-speed squirrel cage induction generator turbines [7]. Squirrel cage induction generators show slight stability margin against voltage drop; consequently, it is necessary to use compensator devices to improve rotor speed stability margin [8]. In order to determine the type and the way of compensation, it is necessary to examine characteristic curves of induction generator.

The absorbed reactive power, slip and slip-torque characteristics of induction machine are shown in Fig. 2(a) and (b) respectively. As it can be observed in these figures, during the normal operation, the generator has a very low slip close to zero, and, in this case, little reactive power is absorbed by generator. But if

* Corresponding author.
 E-mail address: mhkhoban@googlemail.com (M.H. Khooban).

Nomenclature

ω_r	rotor angular speed	i_{ds}, i_{qs}	d-axis and q-axis stator currents
J	moment of inertia	R_s, R_r	stator and rotor resistances
T_m	mechanical torque	ω_S	rotational speed of the reference device
T_e	electrical torque	$\lambda_{ds}, \lambda_{qs}$	d-axis and q-axis stator Flux linkage vectors
v_s	generator stator voltage	$\lambda_{dr}, \lambda_{qr}$	d-axis and q-axis rotor Flux linkage vectors
S	slip	i_{dr}, i_{qr}	d-axis and q-axis rotor currents
S_{cr}	critical slip	ω_r	rotational speed of the generator's rotor
t_{cr}	critical clearing time	L_s, L_r, L_m	stator, rotor and magnetizing inductances
T_{ae}	aerodynamic torque	e_{dr}, e_{qr}	d-axis and q-axis transient voltages
ω_t	rotational speed of wind turbine	P	number of pole pairs
ρ	air density	H_g	inertia constant of the generator
A	area of wind turbine rotor	i_{de}, i_{qe}	d-axis and q-axis STATCOM currents
V_{wind}	speed of wind	L_f, R_f	transformer of STATCOM res. and ind.
C_P	power coefficient	v_{dc}	dc voltage of STATCOM
λ	tip speed ratio	C, R	DC capacitor and resistance
β	pitch angle	α	Phase angle of the STATCOM
H_t	inertia constant	m	modulation index
D_t	wind turbine damping	A, B	system matrices
v_{ds}, v_{qs}	d-axis and q-axis stator voltages	R, Q	LQR matrices

the generator is accelerated, the reactive power absorbed by the generator begins to increase with large gradient. The increase in reactive power absorbed by the generator, will lead to a lack of voltage recovery, after the voltage drop is removed. Lack of prompt voltage profile recovery may also cause rotor speed instability.

In order to analyze the causes of instability, it is necessary to examine characteristics of induction generator more carefully. As shown in Fig. 3(a), in operating points A_1 and E_1 generator slip is S_1 and its voltage is V_1. In these points electrical and mechanical

torques are equal and generator is in stable state. The occurrence of low voltage in power grid, results in a sudden voltage drop at the terminals of the stator from V_1 to V_2. Consequently, the electric torque and absorbed reactive power drop from A_1 to B_1 and from E_1 to F_1 respectively. Since Exciting torque is much higher than electrical torque, generator starts to accelerate and its slip reaches to S_2. Consequently, the electric torque and reactive power characteristics start to move towards C_1 and G_1 respectively. After fault handling and recovery of grid voltage, since the rotor slip still remains high, a great amount of reactive power is absorbed by the stator terminals of generator which leads voltage to be recovered to a point where the voltage is less than V_2 i.e. V_3. In this case operating points of generator are D_1 and H_1. Since, in these points, the electrical torque is more than mechanical torque, the rotor slip gradually decreases, which means reducing the absorption of reactive
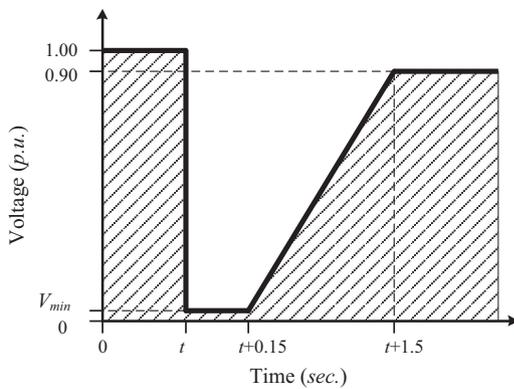

Fig. 1. Example of LVRT requirement to the wind turbine farms [4].
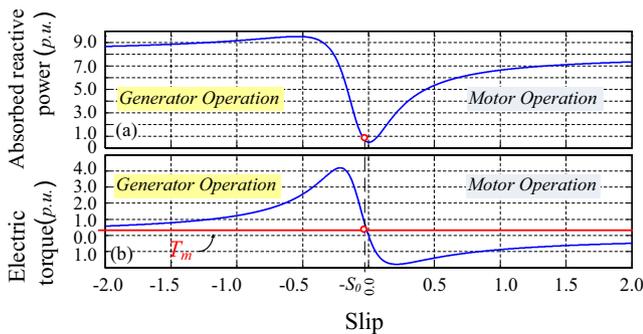

Fig. 2. Characteristics of induction machine (a. reactive power-slip, b. electric torque-slip).
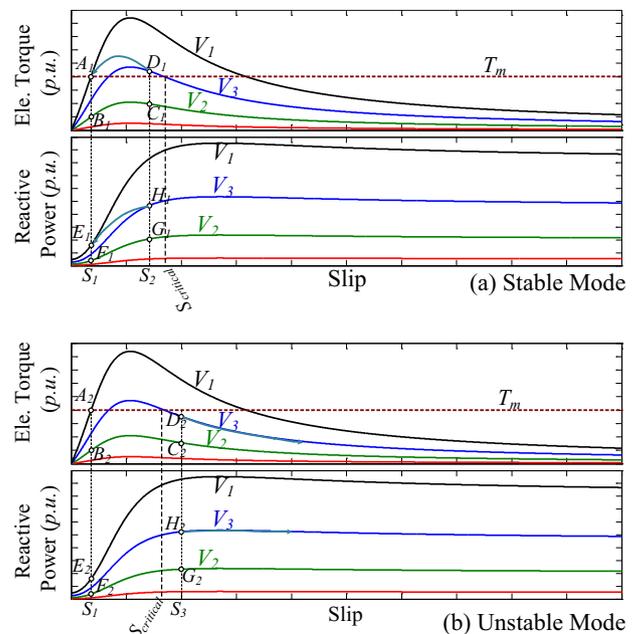

Fig. 3. Characteristics of induction generators when the low voltage occurs (a. stable state, b. unstable state).

power and increasing profile voltage levels. After a while, generator returns to its stable operating point (A_1 and E_1) and maintains its stability.

Considering Fig. 3(b), a condition is discovered in which the low voltage is removed when the rotor slip is S_3. Similar to the previous case, after removing the fault, the operating points are shifted from C_2 to D_2 and G_2 to H_2. In contrast to the previous case, the electric torque is still less than mechanical torque and this leads slip to increase again and more reactive power is absorbed, which reduces the voltage and rotor speed instability will occur.

To determine critical fault clearing time i.e. the maximum fault duration in which the system stability can be maintained, the following equation is used:

$$\frac{d}{dt}S = \frac{1}{J}(T_m - T_e) \tag{3}$$

Therefore,

$$\int_{S_0}^{S_{cr}} dS = \frac{1}{J}(T_m - T_e)\int_0^{t_{cr}} dt \tag{4}$$

So, the critical fault clearing time is:

$$t_{cr} = \frac{J}{T_m - T_e}(S_{cr} - S_0) \tag{5}$$

Aside from the uncertainty of weather forecasts, there is a great concern when integrating wind power into the utility grid is the consequences of grid voltage disturbances. If the grid voltage drops, for instance because one or more of the grid's phases are short-circuited, the electromagnetic torque of the wind generator also drops. But the driving torque, which is the wind, remains unchanged and the resulting imbalance lets the rotor accelerate. Depending on the strength of the wind and the length of the fault, the current in the machine might become high enough to trip the over-current protection system and disconnect from the grid. Regarding this, to ensure power stability, utility grid operators are introducing new rules in their grid codes. These rules state under which circumstances wind farms may disconnect and under which they must continue supplying the grid. To enable wind power plants to meet these new demands, different methods for improving their operational stability have been suggested and are referred to as strategies for low voltage ride through (LVRT) of wind farms.

According to this analysis, in order to improve rotor speed stability margin or to increase critical fault clearing time, using reactive power compensator devices for providing generator with reactive power can be proposed. Also, by reducing the mechanical torque during rotor acceleration its speed can be reduced.

In [9,10], in order to reduce the mechanical torque during acceleration, pitch angle control system is used. References [11,12] used SVC equipment to provide the required reactive power of the generator during acceleration also, STATCOM reactive power compensator is used in [13–15] to provide induction generator with reactive power. In reference [16] a comparison is made between SVC and STATCOM. The result of this comparison shows that for improving reactive power STATCOM is more useful than SVC.

In [17] the authors used a STATCOM with an energy storage system (STATCOM/ESS) to supply the reactive power, and increased the LVRT capability, and also controlled test system via robust control technique. There are a great number of control procedures from intelligent to classic ones [18–22] that have been applied for these cases. In some research activities, optimization algorithms were applied [23–26] and some of them used fuzzy controller [27–29].

The lead article in order to improve LVRT, reactive current injected by controlling the angle of the blades and STATCOM, offered in the form of optimal *LQR* control system is done. The

novelty of this paper is mixed electrical and mechanical parts of wind turbine to improve LVRT capability.

The second part of this article deals with system modeling and in the third part of the proposed control system is designed. The fourth section discusses the simulation results.

Power system modeling

The control system proposed in this paper to evaluate the performance of power system is considered as in Fig. 4. This system includes a squirrel cage induction generator, wind turbine and the STATCOM.

Wind turbine model

Aerodynamic torque by a wind turbine can be expressed by the following equation:

$$T_{ae} = \frac{1}{2\omega_t} \cdot \rho \cdot A \cdot V_{wind}^3 \cdot C_P(\lambda, \beta) \tag{6}$$

Wind turbine performance coefficient (C_p) can be estimated by some functions. A typical function of this kind is expressed in the following equation [9,10]:

$$\begin{cases} C_P(\lambda, \beta) = c_1\left(\frac{c_2}{\lambda_i} - c_3\beta - c_4\right)e^{\frac{-c_5}{\lambda_i}} + c_6\lambda \\ \frac{1}{\lambda_i} = \frac{1}{\lambda + 0.08\beta} - \frac{0.035}{\beta^3 + 1} \end{cases} \tag{7}$$

The coefficients c_1 to c_6 are 0.5176, 116, 0.4, 5, 21, and 0.0068 respectively. If internal inertia of the turbine shaft is ignored, turbine rotational speed is:

$$\dot{\omega}_t = \frac{1}{2H_t}(T_{ae} - D_t\omega_t) \tag{8}$$

Squirrel cage induction generator model

Squirrel cage induction generator referred to dq0 framework by means of dynamic equations can be expressed as following:

$$\begin{cases} v_{qs} = R_s i_{qs} + \omega_s \lambda_{ds} \\ v_{ds} = R_s i_{ds} - \omega_s \lambda_{qs} \\ \dot{\lambda}_{qr} = -R_r i_{qr} - (\omega_s - \omega_r)\lambda_{dr} \\ \dot{\lambda}_{dr} = -R_r i_{dr} + (\omega_s - \omega_r)\lambda_{qr} \end{cases} \tag{9}$$

In these equations, as discussed in [11] the stator flux changes are ignored.

Let some simplifications be done:

$$\begin{cases} e_{dr} = \omega_s \frac{L_m}{L_r}\lambda_{dr} \\ e_{qr} = -\omega_s \frac{L_m}{L_r}\lambda_{qr} \end{cases} \tag{10}$$
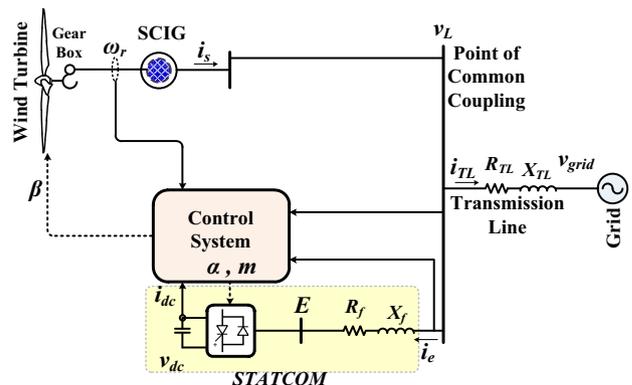

Fig. 4. Model of the system.

We will have:

$$\begin{cases} \dot{e}_{qr} = \frac{-R_r}{L_r}E_{qr} - (\omega_s - \omega_r)e_{dr} + \omega_s r_r\left(\frac{L_m}{L_r}\right)^2 i_{ds} \\ \dot{e}_{dr} = \frac{-R_r}{L_r}E_{dr} + (\omega_s - \omega_r)e_{qr} - \omega_s r_r\left(\frac{L_m}{L_r}\right)^2 i_{qs} \end{cases} \quad (11)$$

Also, the stator voltage will be:

$$\begin{cases} v_{ds} = R_s i_{ds} - \omega_s\left(L_s - \frac{L_m^2}{L_r}\right)i_{qs} + e_{dr} \\ v_{qs} = R_s i_{qs} + \omega_s\left(L_s - \frac{L_m^2}{L_r}\right)i_{ds} + e_{qr} \end{cases} \quad (12)$$

The induction generator rotor speed and electrical torque is expressed as follows:

$$\begin{cases} T_e = \frac{3P\omega_s}{2}(i_{qs}e_{qr} + i_{ds}e_{dr}) \\ \dot{\omega}_r = \frac{P}{2H_g}(T_e - T_{ae}) \end{cases} \quad (13)$$

STATCOM model

STATCOM model is shown in Fig. 5, which includes Transformers, Voltage Source Converter (VSC) and a control system.

Values of active and reactive power exchanged between the STATCOM and the AC transmission system. This exchange is determined by the voltage difference between two sides of the transformer in Fig. 5. If VSC terminals voltage is greater than the AC system voltage, STATCOM produces reactive power; otherwise, reactive power will be consumed by STATCOM. Real power transferred from the AC system to the STATCOM, is well spent for capacitor charging and switching losses. The amount of exchanged power is determined by the phase difference between voltage and ac voltage STATCOM.

STACOM dynamic behavior is described by the following algebraic equations:

$$\dot{i}_{de} = \frac{1}{L_f}\left[(v_{ds} - e_d) - R_f i_{de}\right] + \omega_s i_{qe} \quad (14)$$

$$\dot{i}_{qe} = \frac{1}{L_f}\left[(v_{qs} - e_q) - R_f i_{qe}\right] - \omega_s i_{de} \quad (15)$$

The DC circuit as described by the first order differential equation is:

$$\dot{v}_{dc} = \frac{k}{C}(i_{de}\cos\alpha + i_{qe}\sin\alpha) - \frac{v_{dc}}{RC} \quad (16)$$

And,

$$e_d = kv_{dc}\cos\alpha, \quad e_q = kv_{dc}\sin\alpha \quad (17)$$

STATCOM terminal voltage is equal to e and its value is kv_{dc}. For 12-pulse VSC value of k is equal to $\sqrt{3/8}\,m$.
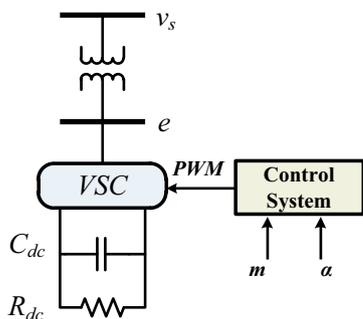
Fig. 5. STATCOM model.

Control system design

State variables describing the system are $x = [\omega_t, \omega_r, e_{dr}, e_{qr}, i_{de}, i_{qe}, v_{dc}]^T$. The first step in designing control systems is the linearization.

$$\Delta\dot{\omega}_t = \frac{1}{2H_t}\left(\left.\frac{\partial T_{ae}}{\partial\beta}\right|^{\omega_t^{(0)}}\Delta\beta + \left.\frac{\partial T_{ae}}{\partial\omega_t}\right|^{\beta^{(0)}}\Delta\omega_t - D_t\Delta\omega_t\right)$$
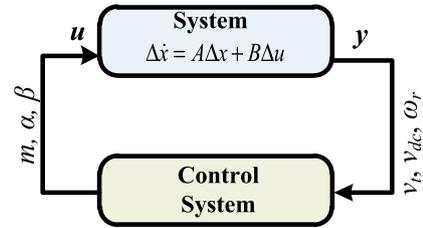
Fig. 6. Control system block diagram for the proposed system.

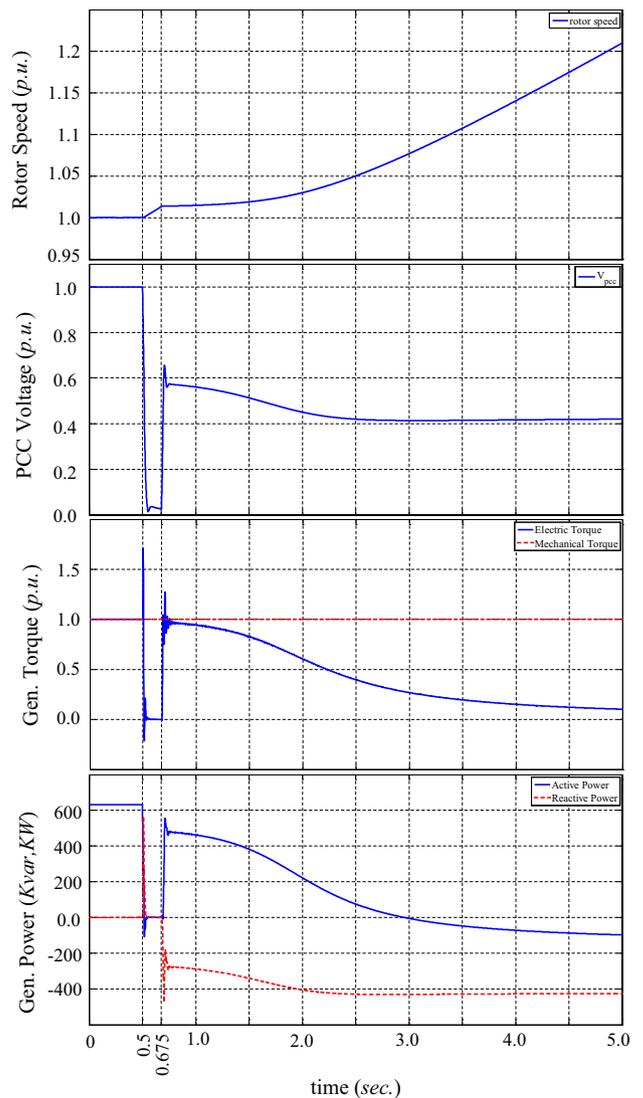Fig. 7. The simulation results of the voltage drop, the system without compensation.

$$\Delta\dot{\omega}_m = \frac{P}{2H_g}\left[i_{ds}^{(0)}\Delta e_{dr} + e_{dr}^{(0)}\Delta i_{ds} + i_{qs}^{(0)}\Delta e_{qr} + e_{qr}^{(0)}\Delta i_{qs}\right.$$
$$\left. -\left(\frac{\partial T_{ae}}{\partial\beta}\bigg|^{\omega_t^{(0)}}\Delta\beta + \frac{\partial T_{ae}}{\partial\omega_t}\bigg|^{\beta^{(0)}}\Delta\omega_t\right)\right]$$

$$\Delta\dot{e}_{qr} = \frac{-R_r}{L_r}(\Delta e_{qr}) - (\omega_s - \omega_r^{(0)})(\Delta e_{dr}) + e_{dr}^{(0)}\Delta\omega_r + \omega_s\frac{R_rL_m^2}{L_r^2}\Delta i_{ds}$$

$$\Delta\dot{e}_{dr} = \frac{-R_r}{L_r}(\Delta e_{dr}) + (\omega_s - \omega_r^{(0)})(\Delta e_{qr}) - e_{qr}^{(0)}\Delta\omega_r + \omega_s\frac{R_rL_m^2}{L_r^2}\Delta i_{qs}$$

$$\Delta\dot{i}_{de} = \frac{1}{L_f}\left[-R_f\Delta i_{de} + \omega_sL_f\Delta i_{qe} + \Delta v_{ds} - \sqrt{\frac{3}{8}}(m^{(0)}\cos\alpha^{(0)}\Delta v_{dc}\right.$$
$$\left. - m^{(0)}v_{dc}^{(0)}\sin\alpha^{(0)}\Delta\alpha + v_{dc}^{(0)}\cos\alpha^{(0)}\Delta m)\right]$$

$$\Delta\dot{i}_{qe} = \frac{1}{L_f}\left[-R_f\Delta i_{qe} - \omega_sL_f\Delta i_{de} + \Delta v_{qs} - \sqrt{\frac{3}{8}}(m^{(0)}\sin\alpha^{(0)}\Delta v_{dc}\right.$$
$$\left. + m^{(0)}v_{dc}^{(0)}\cos\alpha^{(0)}\Delta\alpha + v_{dc}^{(0)}\sin\alpha^{(0)}\Delta m)\right]$$

$$\Delta\dot{v}_{dc} = \frac{\sqrt{\frac{3}{8}}}{C}\left[\Delta m\left(i_{de}^{(0)}\cos\alpha^{(0)} + i_{qe}^{(0)}\sin\alpha^{(0)}\right) + \Delta i_{de}\left(m^{(0)}\cos\alpha^{(0)}\right)\right.$$
$$\left. + \Delta i_{qe}\left(m^{(0)}\sin\alpha^{(0)}\right) - \Delta\alpha\left(m^{(0)}i_{de}^{(0)}\sin\alpha^{(0)} - m^{(0)}i_{qe}^{(0)}\cos\alpha^{(0)}\right)\right]$$
$$- \frac{1}{RC}\Delta v_{dc} \tag{18}$$

Since the purpose of this study is to provide a generator speed stability, in order to facilitate computations STATCOM and stator currents are considered to be equal ($i_s = i_e$). Zero superscript refers to the operating point of the system in steady state.

After linearization, we should design the control system. In this paper, linear quadratic regulator (LQR) optimal control system is used. The desired system with its control system is shown in Fig. 6.

Considering turbine and generator parameters given in the appendix, matrices A and B can be written as following:

$$A = \begin{bmatrix} 19.003 & 0 & 0 & 0 & 0 & 0 & 0 \\ 2766700 & 0 & 4318.5 & 4318.5 & 2986.3 & -2986.3 & 0 \\ 0 & 158.72 & 19.37 & -408 & 153000 & 0 & 0 \\ 0 & 158.72 & -408 & -19.37 & 0 & 153000 & 0 \\ 0 & 0 & 0 & 0 & -10.4124 & 157.079 & -31.5656 \\ 0 & 0 & 0 & 0 & -157.079 & -10.4142 & 0 \\ 0 & 0 & 0 & 0 & 510.31 & 0 & -1000 \end{bmatrix}$$

$$B = \begin{bmatrix} 729.961 & 0 & 0 & 0 & 0 \\ 106270 & 0 & 0 & 0 & 0 \\ 0 & 0 & 0 & 0 & 0 \\ 0 & 0 & 0 & 0 & 0 \\ 0 & -63131 & 0 & 0.0194 & 0 \\ 0 & 0 & -63131 & 0 & 0.0194 \\ 0 & 0 & 0 & 0 & 0 \end{bmatrix}$$

ISE control index as given in the following equation:

$$J = k\int_0^{T_s} e(t)^2 dt \tag{19}$$

However, the index for the desired system outputs v_s, ω_m and is considered v_{dc} is expressed as the following equation:

$$J = k\int_0^{T_s}\frac{1}{2}\left(\Delta\omega_m^2 + \Delta v_{dc}^2 + \Delta e_{dr}^2 + \Delta e_{qr}^2\right)dt \tag{20}$$

Consequently, the matrices Q and R are defined as follows:

$$\begin{cases} Q = 0.5 \times diag(0,1,1,1,0,0,1) \\ R = 0.5 \times eye(5) \end{cases} \tag{21}$$
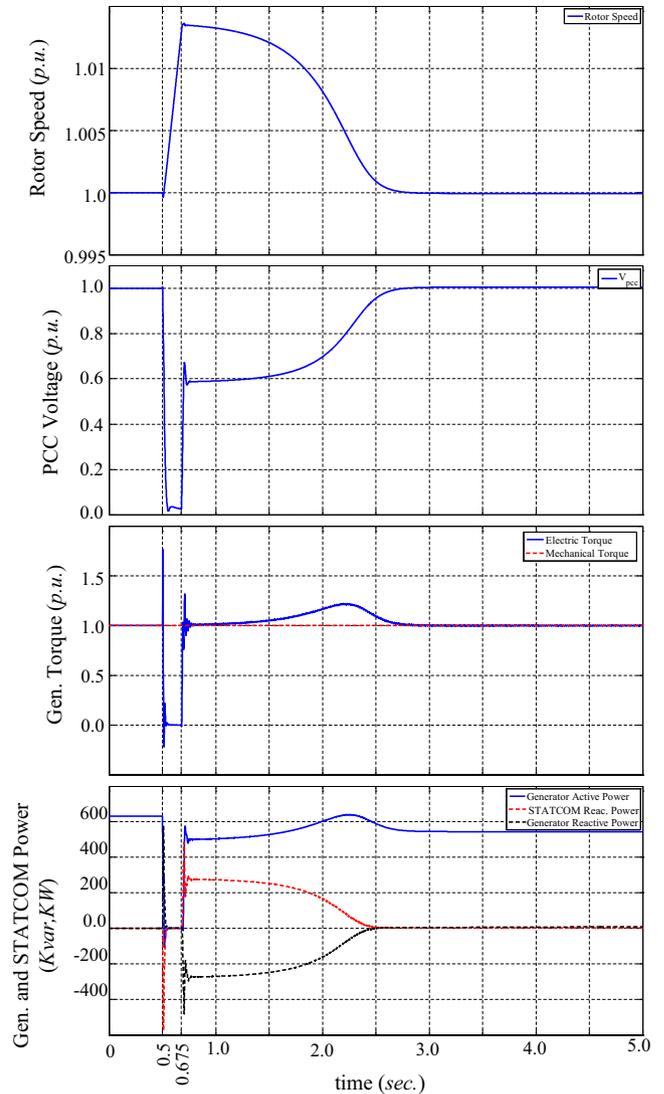

Fig. 8. The simulation results of the voltage drop, the system with STATCOM.

Using structural equation *Riccati* the optimal matrix K is obtained as follows:

$$K = \begin{bmatrix} 23.451 & 0.992 & 0.2392 & 03..78 & 0.2630 & 0.0856 & -8.57\times10^{-5} \\ -3.9527 & -0.1291 & -1.0818 & -0.0786 & -2.3 & -0.0375 & 0.002 \\ -3.4090 & -0.0274 & -0.021 & -1.0523 & -0.0375 & -2.2506 & -7\times10^{-4} \\ 1.21\times10^{-6} & 0 & 0 & 0 & 0 & 0 & 0 \\ 1.04\times10^{-6} & 0 & 0 & 0 & 0 & 0 & 0 \end{bmatrix}$$

Simulation results

Matlab/Simulink software is used to simulate the system that was shown in Fig. 4.

To analyze the system, at first a three-phase voltage to ground fault with a duration of 175 ms is applied to the system at $t = 0.5$ s. As seen in Fig. 7, after fault clearing, system voltage is retrieved but due to high rotor slip which results in large amounts of reactive power absorption, stator terminal voltage cannot be fully retrieved which, in turn, causes rotor speed to become instable. It can be stated that the reason for this instability is the severe loss of electrical torque.

In order to improve system stability, reactive power compensator STATCOM is proposed in this paper. By adding a STATCOM

Fig. 11. Changes in the angle of blades every when the fault occurred during 0.497 s.

Fig. 12. Characteristic changes in critical clearing time in terms of capacity changes STATCOM.

STATCOM reactive current and the pitch angle of the blades is used. In addition to injecting reactive power required during rotor acceleration, the proposed system limits the mechanical torque absorbed by turbine by means of changing rotor blades angle. Simulation results obtained from adding the control system which simultaneously controls STATCOM and pitch angle of the blades are shown in Fig. 10.

In order to further investigate the benefits of the proposed control system, generator rotor speed for various low voltages with different durations is shown in Fig. 10. As seen in this figure, critical clearing time was increased to about 0.497 s. The blades pitch angle for a fault with duration of 0.497 is shown in Fig. 11. It is necessary to note that according to [5], owing to their high inertia, blades pitch angle changing rate is considered to be at most 8 degrees per second.

By increasing capacity of STATCOM, critical clearing time also increases so that the curve changes, this time for the system, with the addition of STATCOM and with STATCOM and pitch angle of the control system is shown in Fig. 12.

As seen in Fig. 12 by increasing the capacity of STATCOM, the rise in critical clearing time in the control system proposed in this paper, it is even more significant.

Conclusions

This paper investigates the role of reactive power compensator STATCOM and presents a control system based on simultaneous control of STATCOM reactive power and pitch angle of rotor blades for improving stability margin of speed of induction generator. As it can be seen in Fig. 12, critical clearing time i.e. maximum fault duration that can occur in the system and yet system is able to return to its steady state, is improved by using STATCOM compensator. In addition, when a STATCOM compensator is used, by increasing STATCOM capacity from 100 to 500 Kvar, critical
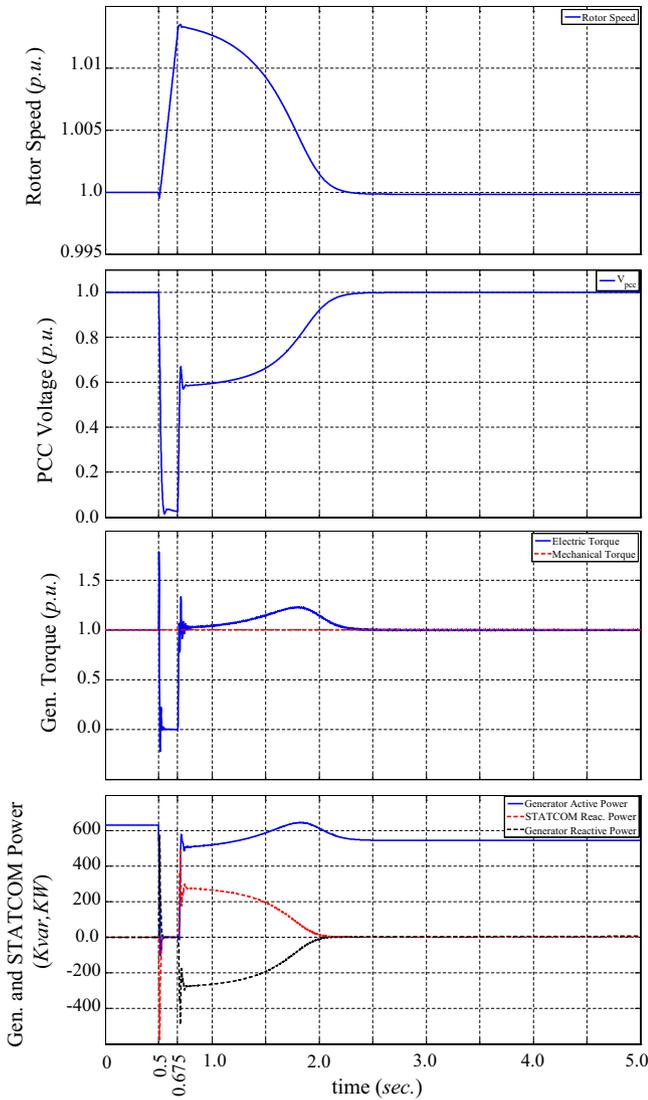

Fig. 9. Simulation results of the system voltage drop compensator STATCOM and STATCOM control the pitch angle of blade.
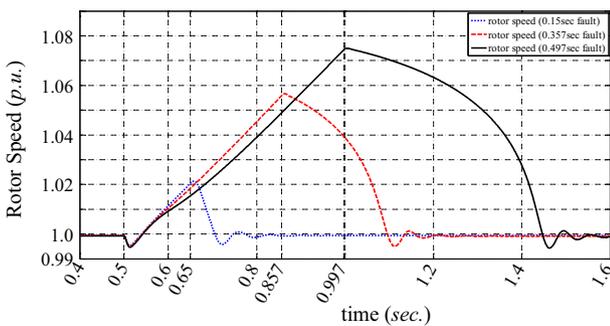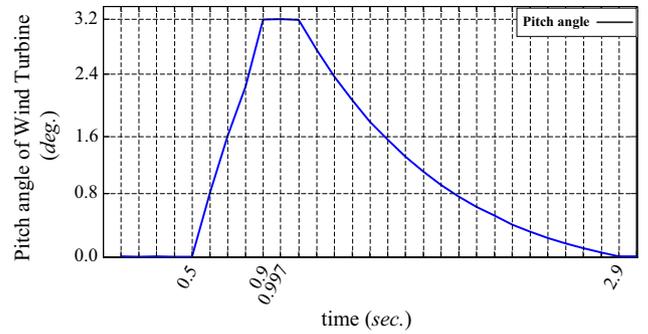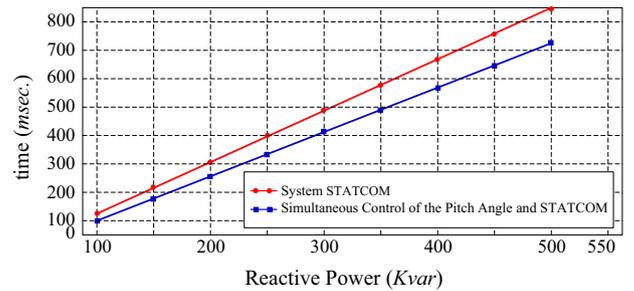

Fig. 10. View of rotor speed control system using STATCOM and pitch angle.

to the system and considering the same three-phase fault as before, as seen in Fig. 8, after retrieving voltage, system returns to its steady state. In fact, in this case, STATCOM prevents electrical torque loss by injecting reactive power required for induction generator (see Fig. 9).

In the next step, as it was explained, for improving stability margin, a control system based on simultaneous control of

Table 1
Wind turbine characteristics [30].

Parameters	Values
Rated power	660 kw
Rotor diagonal	47 m
Swept surface	1735 m^2
Rotor speed	28.5 rpm
Rotation speed of the generator	1515–1650 rpm
Type of generator	Asynchrony 660 kw
Wind speed for power ratings	15 m/s
Minimum and maximum wind speed	4 m/s and 25 m/s
Control system	Pitch control/optislip

Table 2
Wind turbine inertia characteristics.

Parameters	Values
Moment of inertia	1500 kg m^2
Damping constant	1.5 p.u.

Table 3
SCIG characteristics.

Parameters	Values
Moment of inertia	20 kg m^2
Damping constant	0 p.u.
Stator resistance	0.435 Ω
Stator inductance	2.2 mH
Rotor resistance	0.816 Ω
Rotor inductance	2 mH
Magnetize inductance	69.31 mH
Number of poles	4
Nominal voltage	2000 V

clearing time increases from 104 ms to 731 ms while the same rate of increasing the capacity of STATCOM using proposed control system that controls the flow of reactive power of STATCOM and pitch angle of the blades, the critical fault clearing time increases from 158 ms to 843 ms.

Appendix A

*V*47 type of wind turbine used in this article is manufactured by *Vestas* forces. Turbine characteristics are described in Table 1.

Other properties as default, considered as the turbine is shown in Table 2.

Squirrel cage induction generator characteristics are as well as Table 3.

References

[1] Agalgaonkar A, Dobariya C, Kanabar M, Khaparde SA. Optimal sizing of distributed generation in MicroGrid. Presented at the proceedings of IEEE international power india conference, New Delhi; 2006.
[2] Zavadil R, Miller N, Ellis A, Muljadi E. Making connections. IEEE Power Energy Mag 2005:26–37.
[3] Carrasco JM, Franquelo LG, Bialasiewicz JT, Galvan E, Guisado RCP, prats MAM, Leon JI, Alfonso M. Power-electronic system for the grid integration of renewable energy sources: a survey. IEEE Trans Ind Electro 2006;53:1002–16.
[4] Wu B, Lang Y, Zargari N, Kouro S. Power conversion and control of wind energy systems. New Jersey: IEEE Press and John Wiley & Sons; 2011.
[5] Ackermann T. Wind power in power systems. England: John Wiley & Sons Ltd.; 2005.
[6] Salehi V, Afsharnia S, Kahrobaee S. Improvement of voltage stability in wind farm connection to distribution network using FACTS devices. In: 32nd Annual conference on IEEE industrial electronics, IECON 2006, Paris; 2006.
[7] http://www.thewindpower.net/country_en_38_iran.php.
[8] Garcı'a-Gracia M, Comech MP, Salla'n Js, Llombart As. Modelling wind farms for grid disturbance studies. Renew Energy 2008;33:2109–21.
[9] Rajaji L, Kumar C. Neuro fuzzy soft starter for grid integration with pitch regulated wind turbine system. Presented at the international conference on electrical and computer engineering (ICECE); 2008.
[10] Thet AK, Saitoh H. Pitch control for improving the low-voltage ride-through of wind farm. Presented at the transmission & distribution conference & exposition: Asia and Pacific; 2009.
[11] Abdel-Baqi O, Nasiri A. Series voltage compensation for DFIG wind turbine low-voltage ride-through solution. IEEE Trans Energy Convers 2011;26:272–80.
[12] Flannery PS, Venkataramanan G. A fault tolerant doubly fed induction generator wind turbine using a parallel grid side rectifier and series grid side converter. IEEE Trans Power Electron 2008;23.
[13] Ramirez D, Martinez S, Blazquez F, Carrero C. Use of STATCOM in wind farms with fixed-speed generators for grid code compliance. Renew Energy 2012;37:202–12.
[14] Suul JA, Molinas M, Undeland T. STATCOM-based indirect torque control of induction machines during voltage recovery after grid faults. IEEE Trans Power Electron 2010;25:1240–50.
[15] Hossain MJ, Pota HR, Ramos RA. Robust STATCOM control for stabilisation of fixed-speed wind turbines during low voltages. Renew Energy 2011;36:2897–905.
[16] Molinas M, Suul JA, Undeland T. Low voltage ride through of wind farms with cage generators: STATCOM versus SVC. IEEE Trans Power Electron 2008;23:1104–17.
[17] Hossain MJ, Pota HR, Ramos RA. Improved low-voltage-ride-through capability of fixedspeed wind turbines using decentralised control of STATCOM with energy storage system. IET Gener Transm Distrib 2012;6:719–30.
[18] Khalghani MR, Khooban MH. A novel self-tuning control method based on regulated bi-objective emotional learning controller's structure with TLBO algorithm to control DVR compensator. J Appl Soft Comput 2014;24:912–22.
[19] Shamsi-nejad MA, Khalghani MR. DVR control using adaptive PI controller based on human brain learning. In: Proceedings of 17th conference on electric power distribution conference (EPDC), Tehran, Iran; 2012.
[20] Soltanpour MR, Khooban MH, Khalghani MR. An optimal and intelligent control strategy for a class of nonlinear systems: adaptive fuzzy sliding mode. J Vib Control 2014. http://dx.doi.org/10.1177/1077546314526920.
[21] Khalghani MR, Shamsi-nejad MA, Farshad M, Khooban MH. Modifying power quality's indices of load by presenting an adaptive method based on Hebb learning algorithm for controlling DVR. AUTOMATIKA–J Control Measure Electron Comput Commun 2014;55(2).
[22] Sargolzaei A, Moghadasi A, Yen K, Sarwat A. Time-delay analysis on grid-connected three-phase current source inverter based on SVPWM switching pattern. In: IEEE symposium on computational intelligence applications in smart grid (CIASG); 2014. p. 1–5.
[23] Khalghani MR, Shamsi-nejad MA, Khooban MH. DVR control using bi-objective optimization to improve power quality's indices. IET Sci Measure Technol 2014;8(4):203–13.
[24] Shamsi-nejad MA, Zamen MA, Dadgar M, Vahidi T, Khalghani MR. Bi-objective regulating of DVR compensator to modify power quality's indices of load. In: 22nd International conference on electricity distribution (CIRED), Stockholm; June 2013.
[25] Khalghani MR, Shamsi-nejad MA, Beyki K. An intelligent controller for optimal vector control of induction motor. In: IEEE international conference on computer applications and industrial electronics (ICCAIE), Penang, Malaysia; 2011. p. 78–81.
[26] Sargolzaei A, Jamei M, Yen K, Sarwat AI, Abdelghani M. Active/reactive power control of three phase grid connected current source boost inverter using particle swarm optimization. In: Prog Syst Eng. Springer; 2015. p. 141–6.
[27] Shamsi-nejad MA, Khalghani MR, Khooban MH. Determination of optimum hysteresis bandwidth to improve electric machines operation. J Power Technol 2013;93(4).
[28] Sargolzaei A, Yen KK, Abdelghani MN. Time-delay switch attack on load frequency control in smart grid. J Adv Commun Technol 2013;5:55–64.
[29] Heydari-Doostabad H, Keypour R, Eskandarian N, Khalghani MR. New fuzzy control system design for maximum power point tracking of wind turbine. In: 18th Electric power distribution conference (EPDC), Kermanshah, Iran; 2013.
[30] http://www.vestas.com/.